

# Enhancement of Current-Induced Out-of-Plane Spin Polarization by Heavy-Metal-Impurity Doping in Fe Thin Films

T. Yokouchi<sup>✉</sup>\* and Y. Shiomi

*Department of Basic Science, The University of Tokyo, Tokyo 152-8902, Japan*



(Received 20 June 2021; revised 26 August 2021; accepted 14 October 2021; published 1 November 2021)

Current-induced spin polarization in magnets has recently attracted much attention because out-of-plane spin polarization is allowed, as opposed to polycrystalline nonmagnetic heavy metals. We investigate the Pt-impurity-doping dependence of current-induced out-of-plane spin polarization in Fe thin films with the use of magnetocircular dichroism. Current-induced out-of-plane spin polarization is clearly observed and attributed to anomalous spin-orbit torque, in which the spin-orbit torque induced by the spin Hall effect in Fe acts on the magnetic moments of Fe at the surfaces, generating out-of-plane spin polarization. Notably, current-induced out-of-plane spin polarization is significantly enhanced with increasing Pt concentration. Pt impurities with a large spin-orbit interaction induce the extrinsic spin Hall effect of Fe, and consequently, the anomalous spin-orbit torques are enhanced. Our results provide a guiding principle for strengthening current-induced spin polarization in magnets.

DOI: [10.1103/PhysRevApplied.16.054001](https://doi.org/10.1103/PhysRevApplied.16.054001)

## I. INTRODUCTION

Current-induced spin polarization plays an important role in spintronic devices, such as nonvolatile memory devices, in which the magnetization direction is switched by using spin torques arising from current-induced spin polarization [1]. In particular, one of the key factors for efficient control of magnetization is the direction of current-induced spin polarization, which is generally governed by symmetry [2–4]. In the case of nonmagnetic polycrystalline samples, when a charge current flows along the  $x$  direction, the direction of current-induced spin polarization at the top and bottom surfaces is along the  $y$  direction [5,6]. This is because a mirror plane perpendicular to the  $y$  direction forbids spin polarization along the  $x$  and  $z$  directions. In contrast, in ferromagnets, magnetization parallel to the  $x$  direction breaks this mirror symmetry, permitting out-of-plane ( $z$ -direction) spin polarization at the top and bottom surfaces [2–4].

Current-induced out-of-plane spin polarization is important for switching the direction of perpendicular magnetization without an external field [4,7–10]. One example of current-induced out-of-plane spin polarization was reported for magnetic thin films including Permalloy, Ni, and Fe, which is explained by a mechanism termed anomalous spin-orbit torque [3]. Anomalous spin-orbit torque results from the spin torque arising from the spin Hall effect in magnetic metals; as shown in Fig. 1(a), the spin Hall effect in a magnetic metal generates a pure spin current

flowing along the  $z$  direction, and then spins along the  $y$  direction accumulate at the top and bottom surfaces. This spin accumulation generates antidamping spin-orbit torque on magnetic moments given by  $\tau = \tau_{DL} \mathbf{m} \times (\mathbf{m} \times \boldsymbol{\zeta}) = \tau_{DL} \mathbf{m} \times \mathbf{h}_{eff}$ , where  $\tau_{DL}$ ,  $\mathbf{m}$ ,  $\boldsymbol{\zeta}$ , and  $\mathbf{h}_{eff} = \mathbf{m} \times \boldsymbol{\zeta}$  are the coefficient of the antidamping torque, the unit vector of magnetization, the unit vector of spin polarization, and the effective magnetic field, respectively. Since the direction of the effective magnetic field,  $\mathbf{h}_{eff}$ , is perpendicular to the sample plane, the antidamping spin-orbit torque tilts the magnetic moments to the  $z$  direction. In other words, the charge current induces out-of-plane spin polarization. We note that the magnitude of current-induced out-of-plane spin polarization is proportional to the  $x$  component of magnetization ( $M_x$ ), since  $M_x$  breaks the mirror symmetry with respect to the  $x$ - $z$  plane, permitting out-of-plane spin polarization [3].

However, so far, no way to enhance the anomalous spin-orbit torque has been well established, although it is required for efficient current-induced perpendicular magnetization switching without an external magnetic field [4]. To overcome this issue, we focus on heavy-metal-impurity doping. It is well known that the magnitude of the extrinsic spin Hall effect can be enhanced by doping heavy-metal impurities, such as Ir and Pt [11–16]. Hence, a systematic investigation of the dependence of current-induced spin polarization on heavy-metal-impurity concentration is expected to serve as a useful guideline for enhancing current-induced out-of-plane spin polarization.

Here, we investigate the Pt-impurity doping dependence on current-induced spin polarization in Fe thin

\* [yokouchi@g.ecc.u-tokyo.ac.jp](mailto:yokouchi@g.ecc.u-tokyo.ac.jp)

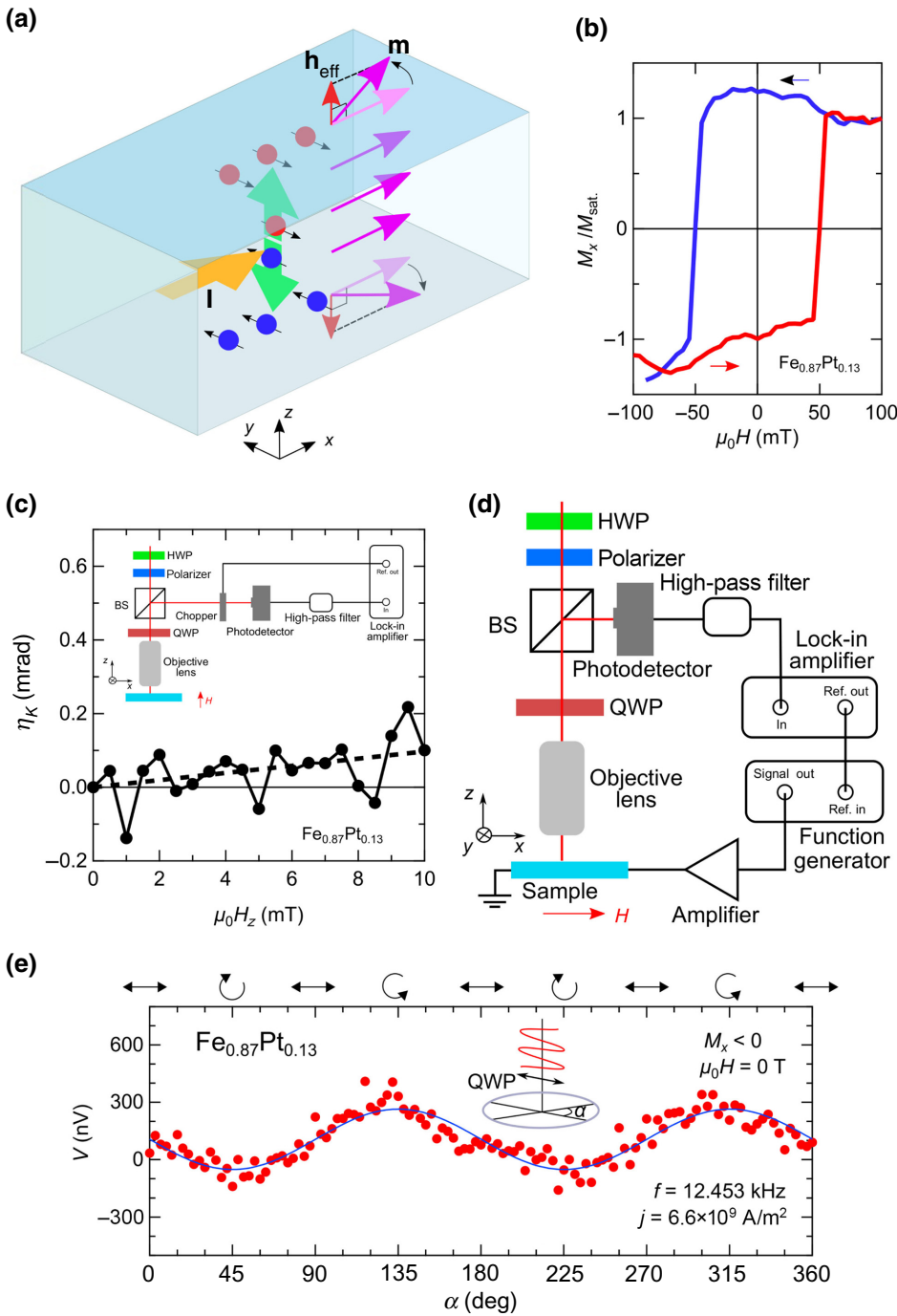


FIG. 1. (a) Schematic of anomalous spin-orbit torque. Charge current (orange arrow) generates a pure spin current (green arrow) flowing along the  $z$  direction, inducing spin accumulation at the top and bottom surfaces. Accumulated spins pointing in the  $y$  direction cause spin-orbit torque (or, equivalently, effective field denoted by red arrows) on magnetic moments of Fe (purple arrow). (b) The  $x$  component of magnetization as a function of magnetic field parallel to the  $x$  direction measured by longitudinal MOKE. (c) Out-of-plane magnetic field ( $H_z$ ) dependence of Kerr ellipticity without applying charge current. Inset represents the experimental setup for this measurement. Black line is a linear fit to data. (d) Schematic diagram of the measurement system for current-induced spin polarization. HWP, BS, and QWP denote half-wave plate, beam splitter, and quarter-wave plate, respectively. (e) Light-polarization dependence of the voltage signal from the photodetector measured by the lock-in amplifier. Here,  $\alpha$  is the angle of the  $\lambda/4$  plate. Symbols  $\leftrightarrow$ ,  $\circlearrowleft$ , and  $\circlearrowright$  represent linearly, right-handed circularly, and left-handed circularly polarized light, respectively.

films. Current-induced out-of-plane spin polarization at the top surface is detected with the use of magnetic circular dichroism (MCD), that is, the difference in absorption between left-handed circularly polarized light (LCP) and right-handed circularly polarized light (RCP) [17–19]. With increasing Pt concentration, the magnitude of the current-induced out-of-plane spin polarization increases. This result indicates the Pt impurities with large spin-orbit coupling enhance the anomalous spin-orbit torques; the enhancement of the extrinsic spin Hall effect in Fe due to Pt doping strengthens the magnitude of the spin-orbit

torque at the top surface, leading to the increase in the tilt of the magnetic moments, and hence the current-induced out-of-plane spin polarization increases.

## II. EXPERIMENT

$\text{Fe}_{1-x}\text{Pt}_x$  thin films with a thickness of 30 nm are deposited on a  $\text{Si}/\text{SiO}_2$  substrate by cosputtering Pt and Fe targets at room temperature. In this process, we place a patterned metal mask in front of the substrate to make films with a rectangular shape of 1.5 mm in length and 500  $\mu\text{m}$

in width. The Pt concentration ( $x$ ) is estimated by using an x-ray fluorescence analyzer (Hitachi, EA6000VX). The in-plane magnetization is measured with the longitudinal magneto-optical Kerr effect (MOKE). To measure current-induced out-of-plane spin polarization, we employ MCD measurements [17–19]. A schematic for the MCD measurements for current-induced out-of-plane spin polarization is shown in Fig. 1(d). Laser light with a wavelength of  $\lambda = 632.8$  nm and power of  $P = 5$  mW is focused at normal incidence onto the  $\text{Fe}_{1-x}\text{Pt}_x$  thin films using a  $50\times$  microscope objective lens. The spot size is approximately  $4\ \mu\text{m}$ , and the position of the spot is set around the center of the films, unless otherwise noted. Since the thickness of thin films (30 nm) is thicker than the penetration depth of the laser light (approximately 14 nm), MCD captures current-induced spin polarization at the top surface. Polarization of the laser light varies by rotating the quarter-wave plate [Fig. 1(d)]. The reflected laser light is detected by a photodetector. We apply an ac current with a frequency of  $f = 12.453$  kHz to the sample ( $x$  direction) and record the voltage signal ( $V_{\text{ac}}$ ) from the photodetector, the frequency of which is the same as the ac current with the use of a lock-in amplifier. Simultaneously, the dc component of the voltage signal ( $V_{\text{dc}}$ ) is also recorded with the use of a voltage meter. The magnetic field is applied parallel to the current direction ( $x$  direction). We also measure the out-of-plane magnetic field dependence of MCD without applying a current. In this case, we modulate laser light by using an optical chopper with a frequency of 7.81 kHz. All measurements are performed at room temperature.

### III. RESULTS AND DISCUSSION

In Fig. 1(b), we show the magnetic field dependence of the  $x$  component of magnetization ( $M_x$ ) normalized by the saturation magnetization ( $M_{\text{sat.}}$ ) for  $\text{Fe}_{0.87}\text{Pt}_{0.13}$ . Here,  $M_x$  is measured without applying charge currents.  $M_x$  exhibits a clear hysteresis loop, indicating that our  $\text{Fe}_{1-x}\text{Pt}_x$  thin films have an in-plane anisotropy. The observed in-plane magnetic anisotropy is consistent with previous reports, in which the origin is attributed to the shape magnetic anisotropy [20–22].

Then, we show the results of MCD measurements. In MCD, the light-polarization dependence of reflectivity is expected to show  $\sin 2\alpha$  dependence, where  $\alpha$  is the angle of the  $\lambda/4$  plate, and its amplitude is proportional to the magnitude of the  $z$  component of spin polarization [17–19]. The light-polarization dependence of  $V_{\text{ac}}$  measured at a current density of  $j = 6.6 \times 10^9 \text{ A/m}^2$  and  $f = 12.453$  kHz for  $\text{Fe}_{0.87}\text{Pt}_{0.13}$  is shown in Fig. 1(e). Here, magnetization is aligned along the  $x$  direction.  $V_{\text{ac}}$  clearly shows the  $\sin 2\alpha$  dependence, as expected for MCD, indicating the presence of the  $z$  component of spin polarization. Moreover, in the present experiment,  $V_{\text{ac}}$  picks up the reflectivity component modulated by the charge current applied to the

sample. Therefore, the observed  $\sin 2\alpha$  dependence of  $V_{\text{ac}}$  indicates the existence of the current-induced  $z$  component of spin polarization.

For quantitative evaluation of current-induced out-of-plane spin polarization, we introduce the Kerr ellipticity ( $\eta_K$ ) by normalizing  $V_{\text{ac}}$  as follows:  $\eta_K = \Delta R/(4R) = (V_{\text{ac,LCP}} - V_{\text{ac,RCP}})/(4V_{\text{dc}})$ , where  $R$ ,  $\Delta R$ ,  $V_{\text{ac,LCP}}$ , and  $V_{\text{ac,RCP}}$  are the reflectivity, the difference between

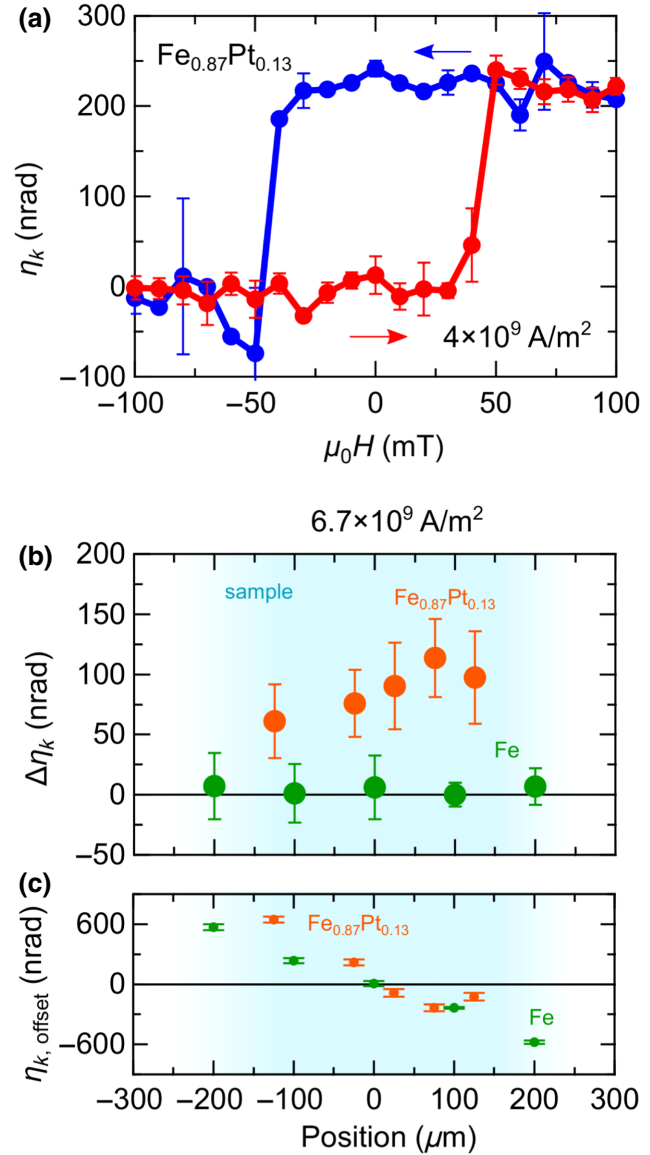


FIG. 2. (a) Kerr ellipticity ( $\eta_K$ ) as a function of magnetic field along the  $x$  direction in  $\text{Fe}_{0.87}\text{Pt}_{0.13}$ . (b) Position dependence of  $\Delta\eta_K$ . Here,  $\Delta\eta_K$  is defined as  $\Delta\eta_K = [\eta_K(+M) - \eta_K(-M)]/2$ , where  $\eta_K(+M)$  and  $\eta_K(-M)$  are the Kerr ellipticity for  $M$  parallel and antiparallel to the  $x$  direction, respectively. Light blue shading represents the sample area. (c) Position dependence of  $H$ -independent offset signal of Kerr ellipticity ( $\eta_{K,\text{offset}}$ ), which is defined as  $\eta_{K,\text{offset}} = [\eta_K(+M) + \eta_K(-M)]/2$ . Error bars correspond to standard deviation.

reflectivity for LCP and RCP, and  $V_{ac}$  for LCP and RCP, respectively. In Fig. 2(a), we show the in-plane magnetic field dependence of  $\eta_K$  measured with  $j = 4.0 \times 10^9 \text{ A/m}^2$ .  $\eta_K$  exhibits a clear hysteresis loop, similar to the hysteresis loop of the in-plane magnetization shown in Fig. 1(b), which indicates that current-induced out-of-plane spin polarization is proportional to in-plane magnetization. This is consistent with the expected behavior of current-induced out-of-plane spin polarization arising from anomalous spin-orbit torque [3], as mentioned in Sec. I. As can be seen from Fig. 2(a),  $\eta_K$  also contains the  $H$ -independent offset signal, which results from the  $z$  component of the Oersted field [3]. Hence, to extract the contribution from the current-induced spin polarization, we define  $\Delta\eta_K$  as  $\Delta\eta_K = [\eta_K(+M) - \eta_K(-M)]/2$ , where  $\eta_K(+M)$  and  $\eta_K(-M)$  are the Kerr ellipticity for  $M$  parallel and antiparallel to the  $x$  direction, respectively.

Then, we investigate the laser-position dependence of current-induced spin polarization. In Fig. 2(b), we show the dependence of  $\Delta\eta_K$  on the position of the laser spot.  $\Delta\eta_K$  is almost constant and maximum around the center of the sample. This is consistent with the anomalous spin-orbit torque mechanism; in the case of current-induced out-of-plane spin polarization arising from anomalous spin-orbit torque, out-of-plane spin polarization appears over the whole area of the sample surface [3]. In addition, to verify that the  $H$ -independent offset signal of Kerr ellipticity ( $\eta_{K,\text{offset}}$ ) results from the  $z$  component of the Oersted field, we investigate the dependence of  $\eta_{K,\text{offset}}$  on the laser-spot position. Here, we define  $\eta_{K,\text{offset}}$  as  $\eta_{K,\text{offset}} = [\eta_K(+M) + \eta_K(-M)]/2$ . Because the  $z$  component of the Oersted field shows sign reversal around the center of the film,  $\eta_{K,\text{offset}}$  is also expected to exhibit a sign change around the center of the film. In fact,  $\eta_{K,\text{offset}}$  shows

a sign change around the center of the film [Fig. 2(c)] as expected, which indicates that the Oersted field originates the  $H$ -independent offset signal of Kerr ellipticity.

We also investigate the current-density dependence of the observed current-induced spin polarization. Figure 3(a) shows the magnetic field dependence of  $\eta_K$  with various current densities in  $\text{Fe}_{0.87}\text{Pt}_{0.13}$  around the center. With increasing current density, the height of the hysteresis loop becomes higher, which is also confirmed from the current-density dependence of  $\Delta\eta_K$  [Fig. 3(b)]. The linear dependence at low current densities is again consistent with anomalous spin-orbit torque. Here, the deviation from the linear relationship in the high-current region ( $>4 \times 10^9 \text{ A/m}^2$ ) might result from the Joule heating effect. Furthermore, we investigate the current-density dependence of the  $H$ -independent offset signal of Kerr ellipticity ( $\eta_{K,\text{offset}}$ ). Since  $\eta_{K,\text{offset}}$  results from the Oersted field,  $\eta_{K,\text{offset}}$  is also expected to be proportional to the current density. In fact, as shown in Fig. 3(c),  $\eta_{K,\text{offset}}$  is proportional to the current density, as expected, which further supports that  $\eta_{K,\text{offset}}$  arises from the Oersted field.

Then, we demonstrate the dependence of current-induced spin polarization on Pt-impurity concentration ( $x$ ). In Figs. 4(a)–4(d), we show the magnetic field dependence of  $\eta_K$  at various Pt concentrations. Fe ( $x = 0$ ) shows no hysteresis loop [Fig. 4(a)], which indicates that the magnitude of current-induced spin polarization is below the noise level of our system. In addition, as shown in Fig. 2(b),  $\Delta\eta_K$  for the Fe film is almost zero over the whole area of the sample. We note that anomalous spin-orbit torque is observed in Fe in a previous report [3]. However, the reported value of anomalous spin-orbit torque in Fe is lower than the detection limit of our setup. With increasing Pt concentration,  $x$ , the height of the hysteresis loop of

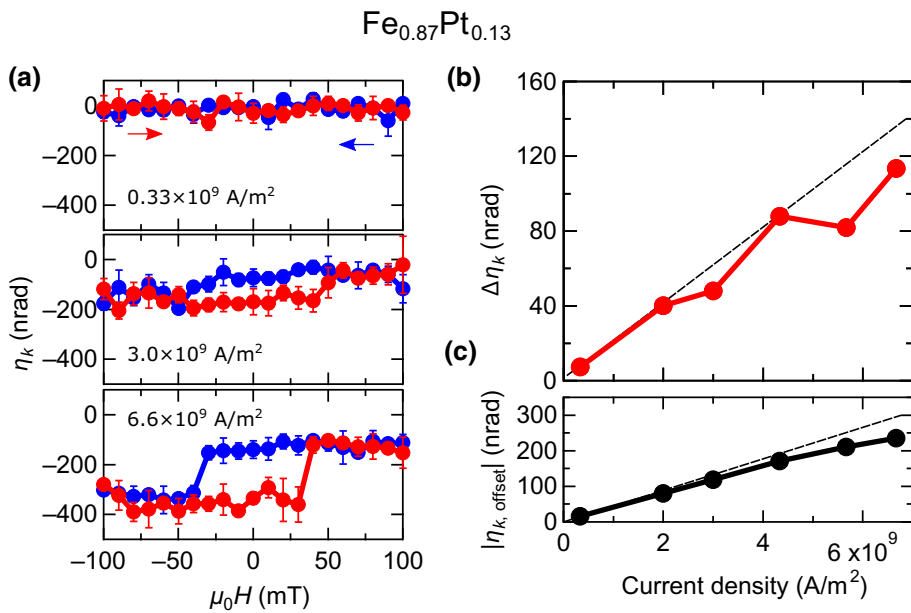


FIG. 3. (a) Kerr ellipticity ( $\eta_K$ ) as a function of magnetic field along the  $x$  direction in  $\text{Fe}_{0.87}\text{Pt}_{0.13}$  at various current densities. Error bars correspond to standard deviation. (b) Current-density dependence of  $\Delta\eta_K$  in  $\text{Fe}_{0.87}\text{Pt}_{0.13}$ . Dashed black line is a guide to the eye. (c) Current-density dependence of the  $H$ -independent offset signal of Kerr ellipticity ( $\eta_{K,\text{offset}}$ ), which is defined as  $\eta_{K,\text{offset}} = [\eta_K(+M) + \eta_K(-M)]/2$ . Dashed black line is a guide to the eye.

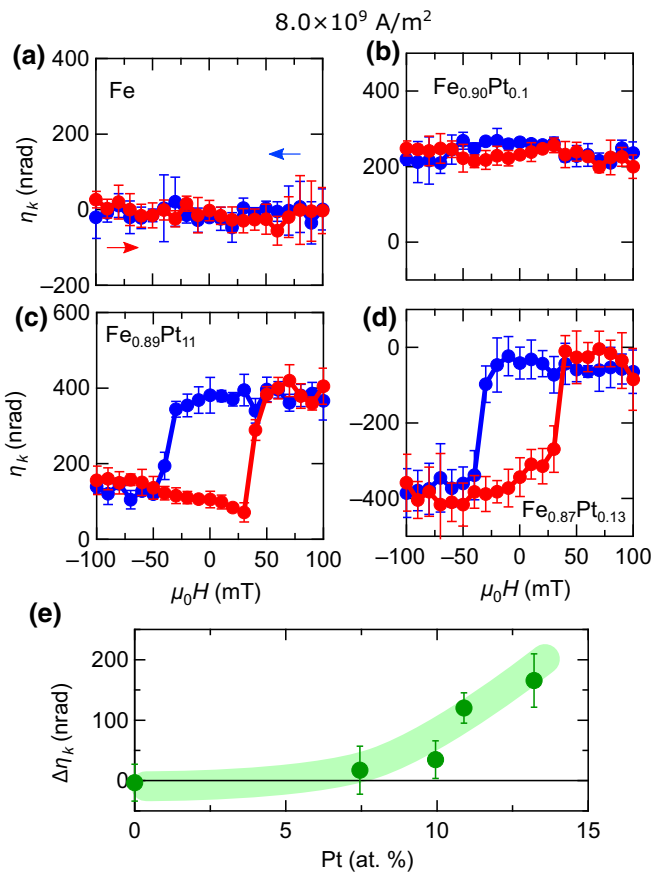


FIG. 4. (a)–(d) Kerr ellipticity ( $\eta_K$ ) as a function of magnetic field along the  $x$  direction at various Pt concentrations ( $x$ ) measured with a current density of  $j = 8.0 \times 10^9 \text{ A/m}^2$ . (e) Pt-concentration dependence of  $\Delta\eta_K$  at a current density of  $j = 8.0 \times 10^9 \text{ A/m}^2$ . Thick green curve is a guide to the eye. Error bars correspond to standard deviation.

$\eta_K$  becomes larger, indicating the enhancement of current-induced out-of-plane spin polarization [Figs. 4(b)–4(d)]. The enhancement of current-induced out-of-plane spin polarization by Pt-impurity doping is also confirmed by the  $x$  dependence of  $\Delta\eta_K$  [Fig. 4(e)];  $\Delta\eta_K$  gradually increases with increasing  $x$ . The enhancement of current-induced out-of-plane spin polarization by Pt-impurity doping is well explained by anomalous spin-orbit torque and the extrinsic spin Hall effect; generally, heavy-metal-impurity doping enhances the extrinsic spin Hall effect because scatterers with strong spin-orbit coupling, which is a source of the extrinsic spin Hall effect, increase [11–16]. Hence, the observed enhancement of current-induced out-of-plane spin polarization by Pt-impurity doping indicates that the extrinsic spin Hall effect in Fe is reinforced by Pt-impurity doping, which leads to the enhancement of anomalous spin-orbit torque, and thus, current-induced out-of-plane spin polarization. We note that the reason why the  $H$ -independent offset of  $\eta_K$  in Figs. 4(a)–4(d) is random is that the position of the laser is not exactly located at the

center; the laser position slightly shifts to the right side in some devices and slightly shifts to the left side in the others, which leads to the random offset of  $\eta_K$ , since the  $H$ -independent offset depends on the position, as shown in Fig. 2(c). We also note that a possible change in the penetration depth due to Pt doping is irrelevant for the observed enhancement of the Kerr ellipticity. Since the penetration depth in Fe is 14 nm, the Kerr ellipticity signal from the bottom surface, which cancels out the Kerr ellipticity signal from the top surface, is less than 1.5% of that from the top surface. Hence, even if this cancellation is reduced by the decrease in penetration depth due to Pt doping, the enhancement of Kerr ellipticity is 1.5% at most, which is much smaller than the experimentally observed enhancement (approximately 380% at least).

Finally, we quantitatively evaluate the magnitude of anomalous spin-orbit torque in the Pt-doped Fe film. To this end, we measure the out-of-plane magnetic field ( $H_z$ ) dependence of Kerr ellipticity ( $\eta_K$ ) without applying a current [see the inset of Fig. 1(c) for the experimental setup]. As shown in Fig. 1(c),  $\eta_K$  is proportional to  $H_z$ , as expected, and  $\eta_K = (0.097 \pm 0.025) \text{ mrad}$  at 10 mT. From this out-of-plane magnetic field dependence of  $\eta_K$ , the effective magnetic field ( $B_{\text{eff}}$ ) due to anomalous spin-orbit torque in Fe\$\_{0.87}\$Pt\$\_{0.13}\$ is estimated to be approximately  $B_{\text{eff}} = (12.3 \pm 3.1) \mu\text{T}$  at  $4 \times 10^9 \text{ A/m}^2$ . In addition, the anomalous spin-orbit torque conductivity ( $\sigma_{\text{ASOT}}$ ), an intrinsic quantity of anomalous spin-orbit torque, is given by  $\sigma_{\text{ASOT}} = (2eM_s t B_{\text{eff}})/\hbar E$ , where  $e$ ,  $M_s$ ,  $t$ ,  $E$ , and  $\hbar$  are the elementary charge, saturation magnetization, film thickness, electric field, and reduced Planck constant, respectively [3]. We obtain  $\sigma_{\text{ASOT}} = (3.1 \pm 0.78) \times 10^3 \Omega^{-1} \text{ cm}^{-1}$  for Fe\$\_{0.87}\$Pt\$\_{0.13}\$. This value is 3.1 times larger than that of the  $\sigma_{\text{ASOT}}$  for Fe reported in Ref. [3].

#### IV. CONCLUSION

We investigate the dependence of current-induced out-of-plane spin polarization on Pt-impurity concentration by means of MCD. The current-induced out-of-plane spin polarization increases with increasing Pt-impurity concentration; this is attributed to the enhancement of the extrinsic spin Hall effect in Fe and the consequent enhancement of anomalous spin-orbit torques. Our findings deepen our understanding of the underlying mechanisms in current-induced out-of-plane spin polarization, as well as providing a guiding principle for enhancing current-induced out-of-plane spin polarization in magnets.

#### ACKNOWLEDGMENTS

The authors are grateful to Dr. Y. Okamura for technical advice on optical experiments. This work is supported by JSPS KAKENHI Grants No. JP21H01794, No. JP21K18890, No. JP20H05153, No. JP20H04631,

No. JP19K22124, No. JP19H05600, No. JP19H02424, and No. JP19K14667.

- 
- [1] A. Manchon, J. Železný, I. M. Miron, T. Jungwirth, J. Sinova, A. Thiaville, K. Garello, and P. Gambardella, Current-induced spin-orbit torques in ferromagnetic and antiferromagnetic systems, *Rev. Mod. Phys.* **91**, 035004 (2019).
- [2] M. Kimata, H. Chen, K. Kondou, S. Sugimoto, P. K. Muduli, M. Ikhlas, Y. Omori, T. Tomita, A. H. MacDonald, S. Nakatsuji, and Y. Otani, Magnetic and magnetic inverse spin Hall effects in a non-collinear antiferromagnet, *Nature* **565**, 627 (2019).
- [3] W. Wang, T. Wang, V. P. Amin, Y. Wang, A. Radhakrishnan, A. Davidson, S. R. Allen, T. J. Silva, H. Ohldag, D. Balzar, B. L. Zink, P. M. Haney, J. Q. Xiao, D. G. Cahill, V. O. Lorenz, and X. Fan, Anomalous spin-orbit torques in magnetic single-layer films, *Nat. Nanotechnol.* **14**, 819 (2019).
- [4] A. Davidson, V. P. Amin, W. S. Aljuaid, P. M. Haney, and X. Fan, Perspectives of electrically generated spin currents in ferromagnetic materials, *Phys. Lett. A* **384**, 126228 (2020).
- [5] J. Sinova, S. O. Valenzuela, J. Wunderlich, C. H. Back, and T. Jungwirth, Spin Hall effects, *Rev. Mod. Phys.* **87**, 1213 (2015).
- [6] F. Hellman, *et al.*, Interface-induced phenomena in magnetism, *Rev. Mod. Phys.* **89**, 025006 (2017).
- [7] S. Fukami, T. Anekawa, C. Zhang, and H. Ohno, A spin-orbit torque switching scheme with collinear magnetic easy axis and current configuration, *Nat. Nanotechnol.* **11**, 621 (2016).
- [8] G. Yu, P. Upadhyaya, Y. Fan, J. G. Alzate, W. Jiang, K. L. Wong, S. Takei, S. A. Bender, L. Te Chang, Y. Jiang, M. Lang, J. Tang, Y. Wang, Y. Tserkovnyak, P. K. Amiri, and K. L. Wang, Switching of perpendicular magnetization by spin-orbit torques in the absence of external magnetic fields, *Nat. Nanotechnol.* **9**, 548 (2014).
- [9] S. H. C. Baek, V. P. Amin, Y. W. Oh, G. Go, S. J. Lee, G. H. Lee, K. J. Kim, M. D. Stiles, B. G. Park, and K. J. Lee, Spin currents and spin-orbit torques in ferromagnetic trilayers, *Nat. Mater.* **17**, 509 (2018).
- [10] Q. Xie, W. Lin, S. Sarkar, X. Shu, S. Chen, L. Liu, T. Zhao, C. Zhou, H. Wang, J. Zhou, S. Gradečák, and J. Chen, Field-Free magnetization switching induced by the unconventional spin-orbit torque from WTe<sub>2</sub>, *APL Mater.* **9**, 051114 (2021).
- [11] Y. Niimi, M. Morota, D. H. Wei, C. Deranlot, M. Basletic, A. Hamzic, A. Fert, and Y. Otani, Extrinsic Spin Hall Effect

Induced by Iridium Impurities in Copper, *Phys. Rev. Lett.* **106**, 12601 (2011).

- [12] Y. Niimi, Y. Kawanishi, D. H. Wei, C. Deranlot, H. X. Yang, M. Chshiev, T. Valet, A. Fert, and Y. Otani, Giant Spin Hall Effect Induced by Skew Scattering From Bismuth Impurities Inside Thin Film CuBi Alloys, *Phys. Rev. Lett.* **109**, 156602 (2012).
- [13] M. Yamanouchi, L. Chen, J. Kim, M. Hayashi, H. Sato, S. Fukami, S. Ikeda, F. Matsukura, and H. Ohno, Three terminal magnetic tunnel junction utilizing the spin Hall effect of iridium-doped copper, *Appl. Phys. Lett.* **102**, 212408 (2013).
- [14] Y. Niimi, H. Suzuki, Y. Kawanishi, Y. Omori, T. Valet, A. Fert, and Y. Otani, Extrinsic spin Hall effects measured with lateral spin valve structures, *Phys. Rev. B* **89**, 054401 (2014).
- [15] R. Ramaswamy, Y. Wang, M. Elyasi, M. Motapothula, T. Venkatesan, X. Qiu, and H. Yang, Experimental Study of Extrinsic Spin Hall Effect in CuPt Alloy, *Phys. Rev. Appl.* **8**, 024034 (2017).
- [16] A. Hrabec, F. J. T. Gonçalves, C. S. Spencer, E. Arenholz, A. T. N'Diaye, R. L. Stamps, and C. H. Marrows, Spin-Orbit interaction enhancement in permalloy thin films by Pt doping, *Phys. Rev. B* **93**, 014432 (2016).
- [17] Y. Liu, J. Besbas, Y. Wang, P. He, M. Chen, D. Zhu, Y. Wu, J. M. Lee, L. Wang, J. Moon, N. Koirala, S. Oh, and H. Yang, Direct visualization of current-induced spin accumulation in topological insulators, *Nat. Commun.* **9**, 2492 (2018).
- [18] Y. Liu, Y. Liu, M. Chen, S. Srivastava, P. He, K. L. Teo, T. Phung, S.-H. Yang, and H. Yang, Current-Induced Out-of-Plane Spin Accumulation on the (001) Surface of the IrMn<sub>3</sub> Antiferromagnet, *Phys. Rev. Appl.* **12**, 064046 (2019).
- [19] P. Seifert, K. Vaklinova, S. Ganichev, K. Kern, M. Burghard, and A. W. Holleitner, Spin Hall photoconductance in a three-dimensional topological insulator at room temperature, *Nat. Commun.* **9**, 331 (2018).
- [20] E. Gu, E. Ahmad, J. Bland, L. Brown, M. Rührig, A. McGibbon, and J. Chapman, Micromagnetic structures and microscopic magnetization-reversal processes in epitaxial Fe/GaAs(001) elements, *Phys. Rev. B* **57**, 7814 (1998).
- [21] E. Ahmad, L. Lopez-Diaz, E. Gu, and J. A. C. Bland, Shape anisotropy induced modification of the magnetization reversal processes in epitaxial microstripes, *J. Appl. Phys.* **88**, 354 (2000).
- [22] K. K. Meng, J. Lu, S. L. Wang, H. J. Meng, J. H. Zhao, J. Misuraca, P. Xiong, and S. von Molnár, Magnetic anisotropies of laterally confined structures of epitaxial Fe films on GaAs (001), *Appl. Phys. Lett.* **97**, 072503 (2010).